Hindawi
International Journal of Aerospace Engineering
Volume 2018, Article ID 3756278, 7 pages
https://doi.org/10.1155/2018/3756278

Research Article

Architecture for Measuring Blade Tip Clearance and Time of Arrival with Multiple Sensors in Airplane Engines

José Miguel Gil-García,[1] **Joseba Zubia**,[2] **and Gerardo Aranguren**[3]

[1]*Department of Electronic Technology, University of the Basque Country, Nieves Cano 12, 01010 Vitoria, Spain*
[2]*Department of Communications Engineering, University of the Basque Country, Alda. Urquijo s/n, 48013 Bilbao, Spain*
[3]*Department of Electronic Technology, University of the Basque Country, Alda. Urquijo s/n, 48013 Bilbao, Spain*

Correspondence should be addressed to José Miguel Gil-García; jm.gil-garcia@ehu.eus

Received 17 January 2018; Accepted 12 April 2018; Published 2 May 2018

Academic Editor: Nicolas Avdelidis

Copyright © 2018 José Miguel Gil-García et al. This is an open access article distributed under the Creative Commons Attribution License, which permits unrestricted use, distribution, and reproduction in any medium, provided the original work is properly cited.

The performance of airplane engines is influenced by the performance of their bladed disks. The loads those engines are under, both internal and external, are the origin of vibrations than can jeopardize their integrity. Traditionally, monitoring of those vibrations has been circumscribed to prototyping and quality tests of manufactured disks. However, the development of nonintrusive sensors and techniques to evaluate the vibration based on those sensors opens the monitoring of full engines, even onboard, to new possibilities. In order to assess the vibrations with these techniques, several sensors should be employed. The distance from the blade tip to the casing (tip clearance) and the time of arrival of a blade in front of the sensor are two parameters that are used as a starting point to characterize the vibrations. A flexible architecture to extract these parameters from the blades of a gas turbine has been developed. The generalization of this architecture is introduced which is able to deal with several sensors simultaneously. An implementation of this architecture has been carried out employing a trifurcated optic sensor, whose working principle is explained. A study of the resources required to implement this architecture on measurements of several optic sensors simultaneously and in parallel is presented. The architecture and measurement method have been validated using signals recorded during the test of the compressor stage with 146 blades on a turbine rig.

1. Introduction

In gas turbine design, the distance between the blade tip and the casing plays an important role in the engine performance [1]. This parameter is known as tip clearance (TC). The smaller this distance is, the more efficient it will be. However, its structural health can be compromised if the blade tip reaches the casing due to deformations in the blades.

During its operation, the disks and the blades of a gas turbine bear vibrations and deformations that can reduce its performance and generate stress becoming the origin of a malfunctioning or damaged engine [2].

Vibration measurement has been used to validate finite element simulation results in the design of new bladed disks or to test the quality of manufactured parts [3], but there are promising application fields in structural health prognosis [4] and clearance active control systems [5].

Traditionally, vibration measurements have been carried out by mounting strain gauges in some critical blades of the disk [6]. These systems are costly to install and fragile due to the harsh operating conditions of the blades. They also modify the airflow characteristics and the blade dynamic response. Furthermore, they do not allow knowing the response of those blades without strain gauges installed in them.

In order to overcome the limitations of strain gauges, methods to calculate the vibrational state of a bladed disk from the data derived from nonintrusive sensors mounted in the casing have been developed. These methods are grouped together under the name of blade tip timing (BTT) or nonintrusive stress measurement systems (NSMS) [7]. They are based on measuring the parameter called time of arrival (ToA). This is the instant at which the blade passes the sensor. Then, it is compared with the time the blade

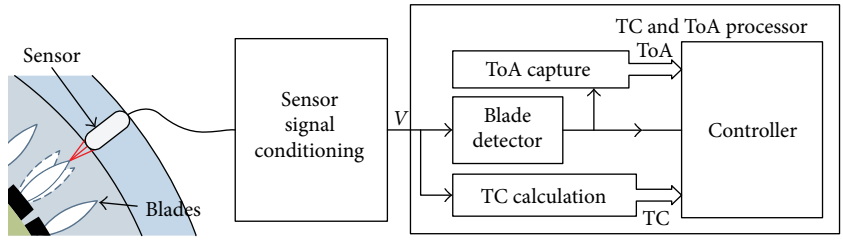

Figure 1: Block diagram of the architecture to extract ToA and TC parameters.

would have passed if no vibration was present. They can also be employed to characterize different modes of engine malfunctioning such as flutter [8] or high-cycle fatigue (HCF) [9].

The type of vibrations can be synchronous and asynchronous. The frequency of synchronous vibrations is a multiple of the rotating disk frequency. For asynchronous vibrations, the amplitude and frequency of the disk response will be calculated up to $\omega_{\max}$ following the equation:

$$\omega_{\max} = \frac{\Omega M}{2}, \tag{1}$$

where M is the number of sensors and Ω the rotating speed [10]. After (1), for a disk rotating at 5000 rpm and for detecting vibrations in the range 0 to 3000 Hz, 72 sensors would be required, which is unfeasible. Proposed methods in the literature try to minimize the number of sensors, still achieving reliable results. Depending on the chosen method, more or less sensors will be needed. In Janicki et al. [11], it is stated that the required number of sensors will be $2 \times m + 2$ where m represents the number of all possible excitations for multiple modes that want to be detected. It gives a usual number of eight sensors. However, the method proposed in Pan et al. [12] needs at least four sensors in order to define the properties of synchronous vibrations and three for the asynchronous ones. A sensor reduction can also be achieved by employing a nonuniform distribution around the casing [13].

In BTT, the most employed sensor technologies are based on capacitance [14], microwave [15], Eddy currents [16], and optical [17] principles. Optic sensors have better bandwidth, resolution, and sensitivity, although they are affected by combustion debris and are not suitable for the engine parts with the highest temperatures.

TC measurement with nonintrusive sensors requires the sensor calibration in order to obtain in the laboratory expressions to relate the distance between the blade tip and the casing to the sensor output. ToA capture is carried out by using level comparators or maximum detectors implemented with external circuits that trigger the capture of high-speed timers [18].

BTT systems can employ an additional sensor that is active once per revolution (OPR) with blade identification and measurement synchronization purposes. Its setup is complex and adds more uncertainty. Under some circumstances, this signal can be derived from the sensors installed to measure the ToA [19].

In most cases found in the literature, the signal processing of the sensor waveforms is carried out by commercial equipment connected to a personal computer. This article presents an architecture capable of extracting the TC and ToA that can be employed to measure several sensors simultaneously. The architecture has been implemented on an electronic instrument that has been validated using the waveforms of a real trifurcated optic sensor tested on a 146-blade compressor in a wind tunnel. In Section 2, the proposed architecture and its adaptation and requirements to measure the optic sensor are described. In Section 3, the test bench to validate the instrument is described. Its implementation is based on a field-programmable gate array (FPGA) type of device. Results will be discussed in Section 4, and in Section 5, the conclusions will be presented.

2. ToA and TC Extraction

2.1. Measuring Architecture. TC and ToA parameter extraction for each sensor is carried out by three synchronized processes during engine operation:

(a) TC calculation

(b) ToA capture

(c) Blade detector

Figure 1 shows the relationship among these processes.

These processes are synchronized by a controller that detects the change of blade event and assigns the TC and ToA values to the blade number that just passed the sensor. Through the calibration fit obtained in the lab, the TC is calculated for each sensor sample and the minimum value registered is stored when the change of blade signal is asserted. That very same instant triggers the capture of ToA by means of embedded timers, saving the design and configuration of external trigger circuitry.

2.2. Optic Sensor Description. In order to assess the feasibility of the proposed architecture, a trifurcated optic sensor recently developed is employed. It was tested on a 146-blade compressor stage mounted on a rig in a wind tunnel [20]. Figure 2 shows the sensor and its response.

The operation principle of the sensor is the intensity modulation of the reflected light. The sensor consists of a bundle of three concentric rings of fibers that is installed in the casing (common leg, left). The central fiber (leg 0) leads a laser beam that will be reflected by the blade and captured

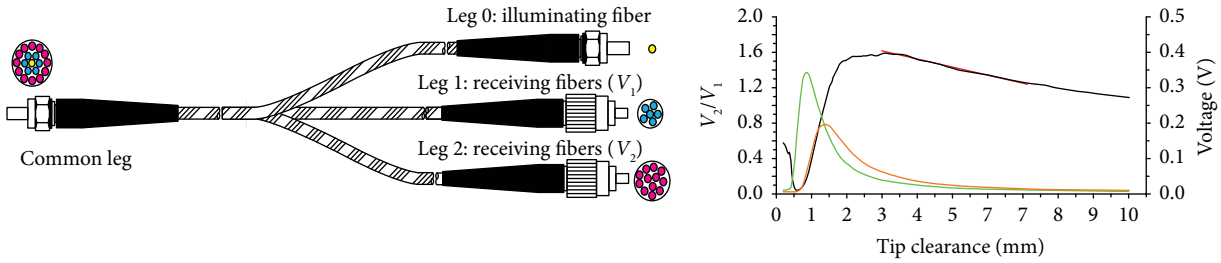

Figure 2: (a) Trifurcated optic sensor diagram. (b) Sensor response (black) over distance (V_1 in green and V_2 in orange).

by the outer concentric rings (blue and magenta). Reflected light is amplified and converted into voltages V_1 and V_2, on the other side (leg 1 and leg 2). Output voltage, V_i, from the ith photodetector will be proportional to the irradiance of the light reaching the photodetector, I_i, the illuminated area in the photodetector, A_i, its responsivity, R_i, and its gain, G_i.

$$V_i = I_i \cdot A_i \cdot R_i \cdot G_i. \tag{2}$$

Besides, the irradiance reaching the photodetector, I_i, will be proportional to the irradiance of the transmitting fiber, I_o, the blade reflectivity, R_{blade}, the losses in the fiber, K_i, the light fluctuations, K_o, and the irradiance captured by the fibers in the outer rings which, in turn, will be a function $F_i(d)$ of the distance, d.

$$I_i = K_o \cdot K_i \cdot R_{blade} \cdot F_i(d). \tag{3}$$

Substituting (3) in (2), the quotient V_2/V_1 is proportional to distance, d, and insensitive to changes in the blade reflectivity or light intensity.

$$\frac{V_2}{V_1} = \frac{K_2 \cdot F_2(d) \cdot A_2 \cdot R_2 \cdot G_2}{K_1 \cdot F_1(d) \cdot A_1 \cdot R_1 \cdot G_1} = K \cdot F(d). \tag{4}$$

As the positive slope in Figure 2(b) (black) is too close to the blades, the part of the curve with a negative slope was used to obtain a calibration fit valid in the 3–7 mm range (red). The calibration equation is represented in (5) ($R^2 = 0.9945$).

$$\frac{V_2}{V_1} = -0.0896 \cdot \mathrm{TC} + 1.8783. \tag{5}$$

Equation (5) was transformed in (6) to obtain the TC from each pair of V_1 and V_2 voltages.

$$\mathrm{TC} = 20.9632 - 11.1607 \cdot q, \tag{6}$$

where q is V_2/V_1. The sensor was tested in a wind tunnel belonging to the company Centro de Tecnologías Aeronáuticas (CTA) that is specialized in aeronautical testing. A compressor stage with a radius of 0.5283 m mounted on a rig was employed. Sensor waveforms were registered on an oscilloscope and processed later on a PC with MATLAB. From all the working points recorded, in this work, the following rotating speeds have been used: 3330, 4601, and 4843 rpm. The disk is supposed to be operated at a maximum of 5000 rpm. The PC processing established that the sensor precision to measure TC was 25 μm. Deflections up to 1 mm were measured.

Table 1: Achievable deflection resolutions (μm).

	10 MHz (μm)	50 MHz (μm)	100 MHz (μm)
3390 rpm	18.8	3.8	1.9
4601 rpm	25.5	5.1	2.5
4843 rpm	26.8	5.4	2.7

2.3. Instrument Requirements. In order to develop a device capable of extracting the TC or ToA that takes advantage of the sensor-proven features, it is needed to set the design requirements in terms of sampling rate, analog to digital converter resolution, and processing method.

2.3.1. Sampling Rate. The system bandwidth is limited by the bandwidth of an employed transimpedance amplifier (Thorlabs PDA-100A) which has a bandwidth of 2.4 MHz for 0 dB gain. Following the Nyquist-Shannon sampling theorem, the sampling rate should be 4.8 MHz at least. However, the resolution to detect a change of blade event would be 0.21 μs which would limit the deflection resolution to roughly 0.058 mm at the most interesting rotation speed (5000 rpm). Hence, a 60 MHz minimum sampling rate is advisable to obtain a minimum deflection resolution of 0.0046 mm at 5000 rpm. Table 1 represents different resolutions achievable with different sampling rates for the available signal waveforms.

2.3.2. ADC Resolution. The maximum ADC input span is 1 V. The ADC resolution should be chosen in such a way that the minimum possible variation of quotient, Δq, should not induce a change in TC (ΔTC), which is higher than the accuracy assigned to the sensor (25 μm). Equation (6) yields that $\Delta q = 0.00224$ holds this condition true.

The voltages determining q, V_1, and V_2 are related by an unknown relationship that takes into account the sensor geometry, amplifier gains, and the different factors affecting the sensor (reflectivity variations, fiber losses, etc.). In order to define the number of bits of the ADC, the maximum Δq variation (and hence, of ΔTC) for simultaneous and opposite increments of one least significant byte (LSB) in both V_1 and

Table 2: Maximum ΔTC (in μm) obtained from the test waveforms for different ADC resolutions.

Rpm	11 bits – LSB = 488 μV (μm)	12 bits – LSB = 244 μV (μm)	13 bits – LSB = 122 μV (μm)
3390	45.6	22.8	11.4
4601	72.6	36.2	18.1
4843	71.9	35.8	17.9

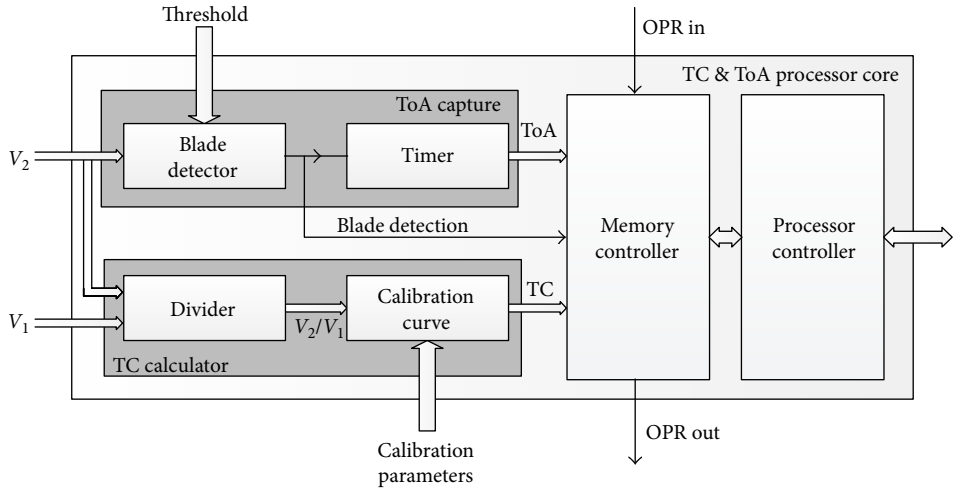

Figure 3: Block diagram of the TC and ToA processor.

V_2 has been computed using the voltage waveforms obtained in the real tests at CTA. By varying the LSB value for different resolutions and checking when the provoked ΔTC is smaller than the accuracy assigned to the sensor, the minimum ADC resolution need can be estimated.

$$\Delta q = \mathrm{MAX}\left[\frac{V_2 + \mathrm{LSB}}{V_1 - \mathrm{LSB}} - \frac{V_2}{V_1}\,;\, \frac{V_2}{V_1} - \frac{V_2 - \mathrm{LSB}}{V_1 + \mathrm{LSB}}\right] < 0.00224. \tag{7}$$

Table 2 represents the computed maximum ΔTC by varying V_1 and V_2 simultaneously and in the opposite direction by just one LSB. At least, 13-bit resolution is needed to achieve an ADC quantization smaller than the sensor accuracy.

2.3.3. TC and ToA Processor. The transmission of the measurement raw data is not feasible due to the high sampling rate required. Thus, if a single 13-bit dual-channel ADC sampling at a 60 MHz rate is chosen, the transmission rate would reach 1560 Mbit/s. It is required to process the ADC samples to extract locally the TC and ToA of each blade.

Implementations of the TC and ToA extraction algorithms based on sequential program flow devices such as microprocessors can barely cope with the processing speed requirements and do not scale. Concurrent logic and pipeline processing suits the FPGA-based implementations the best. The features of an FPGA are also suitable to scale the processing to many sensors. The sequential algorithms designed in MATLAB to detect the change of blade have been redesigned to be adapted to the nature of the FPGA technology [21]. Figure 3 shows the block diagram of the TC and ToA processor.

The *blade detector* block is able to find autonomously in real time the instants at which a blade passes without external hardware nor previous knowledge of the rotating speed. It uses V_2 because of its higher dynamic range. The *TC calculator* block computes in a pipeline fashion the TC for each V_1 and V_2 voltage pair using (6) as the calibration fit. The *memory controller* monitors TC to keep the minimum one over one blade and, when the blade detection signal is asserted, it stores TC and ToA in the memory position assigned to the current blade so that it can be read by another processor.

In the wind tunnel, there was no external signal available that could be asserted each time the disk passes an absolute origin in each revolution (OPR signal). To overcome this problem, the synchronization among simultaneous readings of different sensors by the TC and ToA processors requires that each of them knows when the disk is at the origin and, once at it, which sensor number they are facing. The second parameter can be configured from the *processor controller*, along with others like the calibration parameters and total number of blades. Additionally, one of the cores should be configured as a master (by assigning a #0 blade position). It will assert an *OPR out* signal in each revolution confirming that the relative origin position is reached. The rest of the processors wait for the assertion of the *OPR in* signal to start storing the processed parameters in the memory position assigned to the blade they are facing in that moment. The block diagram of the synchronization is shown in Figure 4.

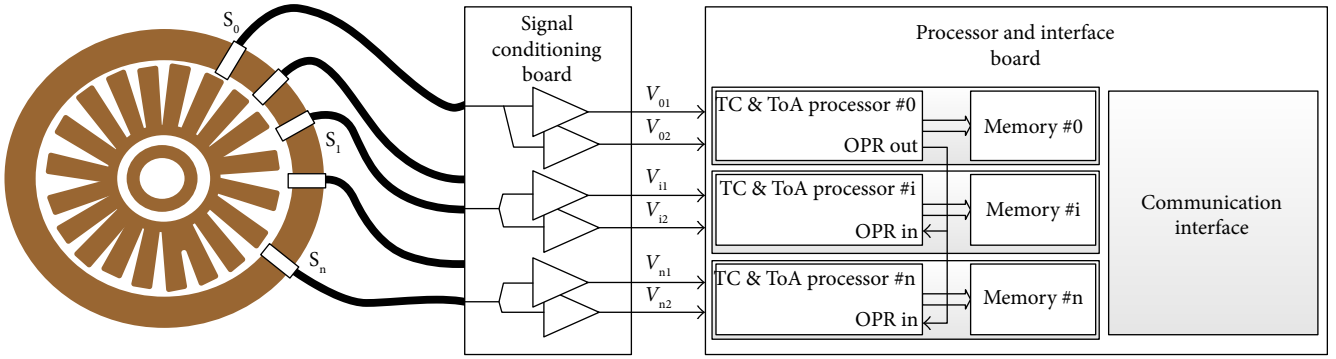

Figure 4: Block diagram showing the measurement synchronization of several sensors.

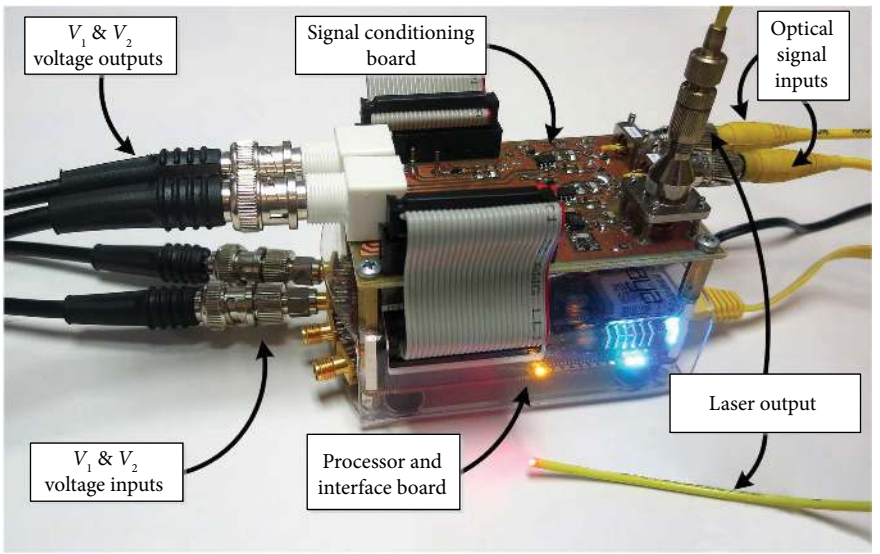

Figure 5: TC and ToA measuring device implementation.

3. Implementation and Tests

Rather than developing an ad hoc instrument, an FPGA development platform called Red Pitaya has been used to implement and validate the design of the instrument. It fulfills the requirements mentioned above as it features a 14-bit dual-channel ADC with ±1 V input range and 125 MHz sampling rate. Figure 5 shows the completed instrument.

The hardware platform features an FPGA model XC7Z010. The instantiated processor has the capacity to store the parameters of 256 blades. Table 3 shows the FPGA resources employed to instantiate one single TC and ToA processor.

Table 4 shows the utilization percentages of the resources offered by the smallest FPGA models of the stated families regarding the implementation requirements of one single TC and ToA processor core.

It can be deduced that a custom board to measure several sensors can be accomplished by an average-size FPGA. The limit is established by the amount of I/O blocks available in the FPGA, as each block will be connected to each dual-channel AD converter that samples a sensor.

Table 3: FPGA resources needed to implement one single TC and ToA processor.

	Slice LUTs	Slice registers	Block RAM	DSP	I/O pins
Implementation	2268	3138	1	2	29

4. Results

One single core measuring one sensor was originally validated by connecting the ADC inputs to the output of two synchronized waveform generators. These were playing the samples recorded in the real tests. The validation was carried out with the three sets of rotation speeds mentioned. The TC processed by the instrument differed from the value obtained by the PC processing less than 1.8% in the worst case [22]. Likewise, the optic sensor deviated a 2.2% in the worst case from the discharge sensor employed in the real tests [20].

Table 4: Utilization percentage of the available resources in different FPGA families.

FPGA family	FPGA model	Slice LUTs	Slice registers	Block RAM	DSP
ZYNQ	XC7Z010dg400	15.5%	8.9%	1.7%	2.5%
ARTIX-7	XC7A035tcgp236	13.1%	7.5%	2.0%	2.2%
KINTEX-7	XC7K070tfbg584	6.6%	0.4%	0.7%	0.8%
VIRTEX-7	XC7V585tffg1157	0.7%	0.4%	0.1%	0.1%

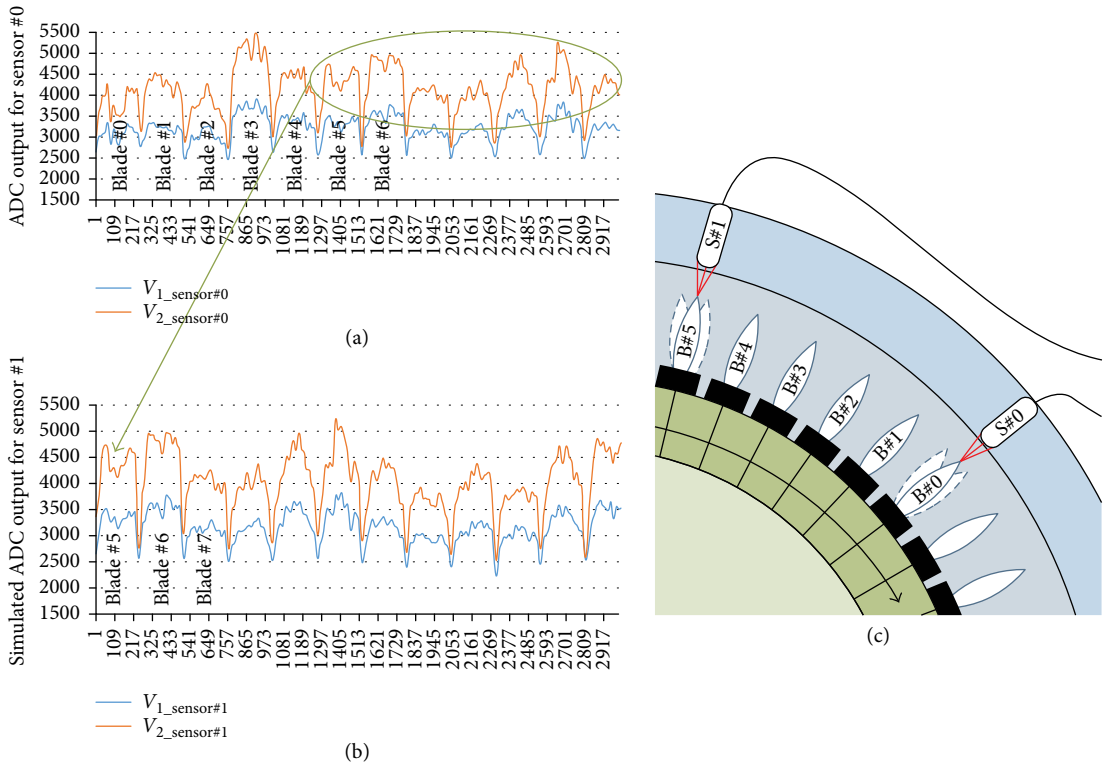

Figure 6: V_1 and V_2 waveforms for two sensors: (a) master sensor (S#0) at blade #0; (b) slave sensor (S#1) facing blade #5; (c) two-sensor simulation setup.

Due to the lack of real simultaneous data from different sensors during the sensor validation tests, waveform files with shifted blades from the original waveform files have been generated to simulate the simultaneous capture of several sensors. Thus, samples corresponding to V_1 and V_2 of the first five blades have been deleted and appended to the end of the file (see Figure 6). With those two sets of files (original and shifted), a simulation featuring two cores has been run. The first core was configured with blade number 0, and it processed the original waveforms. The second core was configured with blade number 5, and it processed the waveform files with samples forwarded by five blades. This would be equivalent to measure a sensor installed in five blades backwards in the rotating direction (Figure 6(c)). Because the signals were actually the same, after running the simulation, the memory contents corresponding to both processors were identical. This validates the synchronization between the processors by means of the OPR signal.

5. Conclusions

An electronic architecture proposed to extract the TC and ToA parameters for each blade of a compressor stage has been implemented. The architecture implementation has been based on the waveforms obtained from a trifurcated optic sensor. Minimum requirements on the electronics needed to measure the TC and ToA have been provided. The implementation takes advantage of the parallel processing capabilities of the FPGAs to measure several sensors simultaneously. The proposed architecture can be adapted to other types of sensors adjusting the *blade detector* block and the *TC calculator* block. This implementation simplifies the hardware, as it does not require external signals to trigger the ToA capture. An internal synchronization signal is generated. It is used as a relative time origin to all possible sensors installed around the casing and their processors. This signal allows that the extracted parameters from each blade passing a given sensor can be stored in analog memory

positions in each processor core, maintaining a coherent representation throughout the system.

Data Availability

All files involved in this work are available upon request for further inspection.

Conflicts of Interest

The authors declare that they have no conflicts of interest.

Acknowledgments

This work has been funded in part by the Fondo Europeo de Desarrollo Regional (FEDER), by the Ministerio de Economía y Competitividad under project TEC2015-638263-C03-1-R, and by the Gobierno Vasco/Eusko Jaurlaritza under projects IT933-16 and ELKARTEK (KK-2016/0030 and KK-2016/0059).

References

[1] D. E. Holeski and S. M. Futral Jr., *Effect of Rotor Tip Clearance on the Performance of a 5-Inch Single-Stage Axial-Flow Turbine*, NASA, Cleveland, OH, USA, 1968.

[2] M. P. Castanier and C. Pierre, "Modeling and analysis of mistuned bladed disk vibration: current status and emerging directions," *Journal of Propulsion and Power*, vol. 22, no. 2, pp. 384–396, 2006.

[3] A. Pezouvanis, G. Janicki, A. Pieronczyk et al., "Turbocharger blade vibration: measurement and validation through laser tip-timing," in *10th International Conference on Turbochargers and Turbocharging*, pp. 173–181, London, UK, 2012.

[4] M. Woike, A. Abdul-Aziz, N. Oza, and B. Matthews, "New sensors and techniques for the structural health monitoring of propulsion systems," *The Scientific World Journal*, vol. 2013, Article ID 596506, 10 pages, 2013.

[5] S. Lattime and B. Steinetz, "Turbine engine control systems: current practices and future directions," in *38th AIAA/ASME/SAE/ASEE Joint Propulsion Conference & Exhibit*, Indianapolis, Indiana, July 2002.

[6] P. Russhard, "The rise and fall of the rotor blade strain gauge," in *Vibration Engineering and Technology of Machinery. Mechanisms and Machine Science, vol 23*, J. Sinha, Ed., Springer, Cham, Manchester, UK, 2014.

[7] R. Szczepanik, E. Rokicki, R. Rzadkowski, and L. Piechowski, "Tip-timing and tip-clearance for measuring rotor turbine blade vibrations," *Journal of Vibration Engineering & Technologies*, vol. 2, no. 5, pp. 395–406, 2014.

[8] V. Georgiev, M. Holík, K. Václav et al., "The blade flutter measurement based on the blade tip timing method," in *Proceedings of the 15th WSEAS international conference on Systems*, Corfu Island, Greece, 2011.

[9] P. Tappert, M. Marcadal, and A. von Flotow, "The last few minutes prior to a fatigue blade failure in an axial compressor: observations of blade vibration and blade lean," in *2007 IEEE Aerospace Conference*, Big Sky, MT, USA, March 2007.

[10] S. Heath and M. Imregun, "A review of analysis techniques for blade tip-timing measurements," in *ASME 1997 International Gas Turbine and Aeroengine Congress and Exhibition*, Orlando, FL, USA, June 1997.

[11] G. Janicki, A. Pezouvanis, B. Mason, and M. K. Ebrahimi, "Turbine blade vibration measurement methods for turbocharges," *American Journal of Sensor Technology*, vol. 2, no. 2, pp. 13–19, 2014.

[12] M. Pan, Y. Yang, F. Guan, H. Hu, and H. Xu, "Sparse representation based frequency detection and uncertainty reduction in blade tip timing measurement for multi-mode blade vibration monitoring," *Sensors*, vol. 17, no. 8, p. 1745, 2017.

[13] Z. Hu, J. Lin, Z.-S. Chen, Y.-M. Yang, and X.-J. Li, "A non-uniformly under-sampled blade tip-timing signal reconstruction method for blade vibration monitoring," *Sensors*, vol. 15, no. 2, pp. 2419–2437, 2015.

[14] C. Lawson, *Capacitance tip timing techniques in gas turbines, [Ph.D. thesis]*, Cranfield University, Bedford, UK, 2003.

[15] M. Violetti, A. K. Skrivervik, Q. Xu, and M. Hafner, "New microwave sensing system for blade tip clearance measurement in gas turbines," in *2012 IEEE Sensors*, Taipei, Taiwan, October 2012.

[16] D. Cardwell, K. S. Chana, and P. Russhard, "The use of eddy current sensors for the measurement of rotor blade tip timing - sensor development and engine testing," in *Proceedings of the ASME turbo Expo 2008: Power for Land, Sea and Air*, Berlin, Germany, June 2008.

[17] S. Cao, F. Duan, and Y. Zhang, "Measurement of rotating blade tip clearance with fibre-optic probe," *Journal of Physics: Conference Series*, vol. 48, pp. 873–877, 2006.

[18] R. Przysowa and K. Kazmierezak, "Triggering methods in blade tip-timing systems," in *International Conference on Vibration Engineering and Technology of Machinery VETOMAC XII*, Warsaw, Poland, 2016.

[19] P. Russhard, "Derived once per rev signal generation for blade tip timing systems," in *IET & ISA 60th International Instrumentation Symposium 2014*, London, UK, June 2014.

[20] I. García, J. Beloki, J. Zubia, G. Aldabaldetreku, M. Illarramendi, and F. Jimenez, "An optical fiber bundle sensor for tip clearance and tip timing measurements in a turbine rig," *Sensors*, vol. 13, no. 6, pp. 7385–7398, 2013.

[21] J. M. Gil-García, I. García, J. Zubía, and G. Aranguren, "Blade tip clearance and time of arrival immediate measurement method using an optic probe," in *2015 IEEE Metrology for Aerospace (MetroAeroSpace)*, Benenvento, Italy, June 2015.

[22] J. M. Gil-García, A. Solís, G. Aranguren, and J. Zubia, "An architecture for on-line measurement of the tip clearance and time of arrival of a bladed disk of an aircraft engine," *Sensors*, vol. 17, no. 10, p. 2162, 2017.

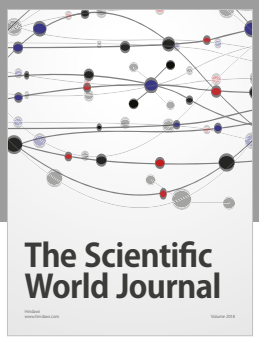

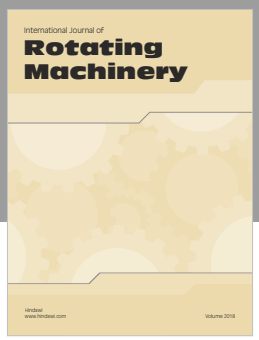

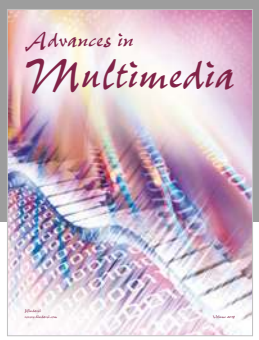

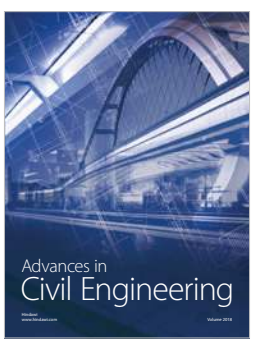

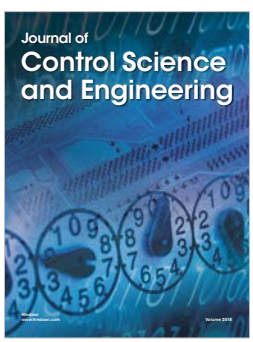

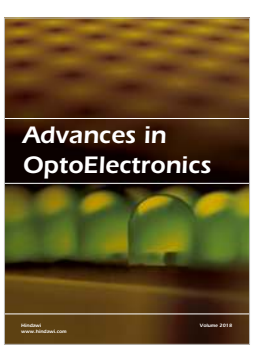

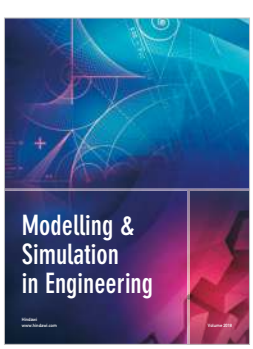

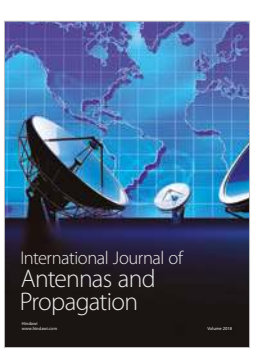

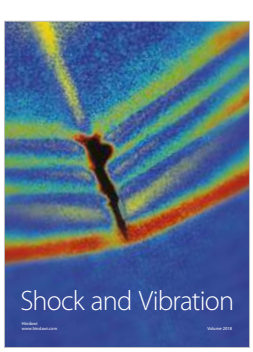

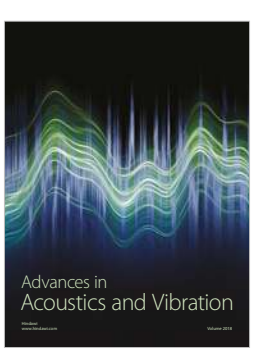

Hindawi

Submit your manuscripts at
www.hindawi.com